
# Dual Nicotinamide Phosphoribosyltransferase and Epidermal Growth Factor Receptor Inhibitors for the Treatment of Cancer

Wanheng Zhang, Kuojun Zhang, Yiwu Yao, Yunyao Liu, Yong Ni, Chenzhong Liao, Zhengchao Tu, Yatao Qiu, Dexiang Wang, Dong Chen, Lei Qiang, Zheng Li, Sheng Jiang

PII: S0223-5234(20)30994-6

DOI: https://doi.org/10.1016/j.ejmech.2020.113022

Reference: EJMECH 113022

To appear in: *European Journal of Medicinal Chemistry*

Received Date: 18 July 2020

Revised Date: 17 October 2020

Accepted Date: 11 November 2020

Please cite this article as: W. Zhang, K. Zhang, Y. Yao, Y. Liu, Y. Ni, C. Liao, Z. Tu, Y. Qiu, D. Wang, D. Chen, L. Qiang, Z. Li, S. Jiang, Dual Nicotinamide Phosphoribosyltransferase and Epidermal Growth Factor Receptor Inhibitors for the Treatment of Cancer, *European Journal of Medicinal Chemistry*, https://doi.org/10.1016/j.ejmech.2020.113022.

# Dual Nicotinamide Phosphoribosyltransferase and Epidermal Growth Factor Receptor Inhibitors for the Treatment of Cancer

Wanheng Zhang[a,#], Kuojun Zhang[a,#], Yiwu Yao[a,#], Yunyao Liu[a,#], Yong Ni[a], Chenzhong Liao[b], Zhengchao Tu[c], Yatao Qiu[a], Dexiang Wang[a], Dong Chen[a], Lei Qiang [a], Zheng Li[d,]*, Sheng Jiang[a,]**

[a]State Key Laboratory of Natural Medicines, Jiangsu Key Laboratory of Drug Design and Optimization and Department of Medicinal Chemistry, China Pharmaceutical University, Nanjing, 210009, China

[b]School of Biological and Medical Engineering, Hefei University of Technology, Hefei, 230009, China

[c]Guangzhou Institutes of Biomedicine and Health, Chinese Academy of Sciences, Guangzhou 510530, China

[d]Center for Bioenergetics, Houston Methodist Research Institute, 6670 Bertner, Houston, Texas 77030, United States

**Abstract:** Multitarget drugs have emerged as a promising treatment modality in modern anticancer therapy. Taking advantage of the synergy of NAMPT and EGFR inhibition, we have developed the first compounds that serve as dual inhibitors of NAMPT and EGFR. On the basis of CHS828 and erlotinib, a series of hybrid molecules were successfully designed and synthesized by merging of the pharmacophores. Among the compounds that were synthesized, compound **28** showed good NAMPT and EGFR inhibition, and excellent *in vitro* anti-proliferative activity. Compound **28**, which is a new chemotype devoid of a Michael receptor, strongly inhibited the proliferation of several cancer cell lines, including H1975 non-small cell lung cancer cells harboring the $EGFR^{L858R/T790M}$ mutation. More importantly, it imparted significant *in vivo* antitumor efficacy in a human NSCLC (H1975) xenograft nude mouse model. This study provides promising leads for the development of novel antitumor agents and valuable pharmacological probes for the assessment of dual inhibition in NAMPT and EGFR pathway with a single inhibitor.

**Keywords**: NAMPT, EGFR, multitarget drugs, dual inhibitor, antiproliferative activity, antitumor efficacy

## 1. Introduction

Cancer is a multifactorial disease associated with dysregulation of multiple genes and cellular signaling pathways. Traditionally targeted therapies that are designed to act specifically on a single oncogenic target often have limited benefits to cancer patients. Rationally, simultaneous modulation of a network of cancer-related targets could be an effective therapeutic approach, and would lead to extensive research and application of specific drug combinations. However, the employment of drug cocktails has some shortcomings and weaknesses, including complex and unpredictable pharmacokinetic properties, potential drug-drug interactions, and poor patient compliance.[1, 2] In an attempt to overcome these disadvantages, a single molecule with multiple targets has captured considerable attention and emerged as an important treatment modality in modern cancer therapy.[3, 4] Thus, multi-targeted drugs can simultaneously and often synergistically target different signaling pathways implicated in the disease resulting in additional effects and better efficacy. In addition, such drugs can have the advantage of concurrent pharmacokinetic profiles, minimized drug-drug interactions and reduced toxicity.

Metabolic alterations are a prototypical hallmark of tumor development which has become an active research area for cancer treatment.[5] Among these targets, nicotinamide adenine dinucleotide (NAD) metabolism has attracted much attention due to its indispensable role in supporting cancer cell proliferation.[6] NAD is a critical component involved in multiple cellular energy-generating and signaling transduction processes and ultimately determining cellular fate. In mammalian cells, NAD can be

synthesized mainly through four pathways: (i) *de novo* biosynthesis employing tryptophan as starting material, (ii) the primary salvage pathway starting from nicotinamide (NAM), and two alternative salvage pathways using (iii) nicotinic acid (NA) and (iv) nicotinamide riboside (NR) as precursors, respectively.[7] Since the NAM-dependent process enables the efficient recycling of NAM by NAD-consuming enzymes such as sirtuins and poly-ADP-ribose polymerases (PARPs), this pathway is the major source for the replenishment and maintenance of NAD.[8] Nicotinamide phosphoribosyltransferase (NAMPT) is the rate-limiting enzyme responsible for the conversation of NAM into nicotinamide mononucleotide (NMN) and the subsequent synthesis of NAD.[9, 10] Because of the uncontrolled and rapid proliferation, cancer cells have much higher energy demand and elevated expression or activity of PARPs and sirtuin than normal cells. In addition, cancer cells have an apparent increase of reactive oxygen species (ROS). NAD and its reduced form NADH contribute to maintaining redox balance of the tumor microenvironment to prevent cells from the oxidative injury.[11, 12] Cancer cells that consume more NAD and are more dependent on NAD-mediated events are more susceptible to NAMPT inhibition than normal cells.[13] Normal cells can use an alternative nicotinic acid phosphoribosyltransferase (NAPRT)-mediated pathway for NAD synthesis from nicotinic acid (NA), thereby protecting themselves from NAMPT inhibition,[14, 15] while most cancer cells lack NAPRT activity.[16, 17] NAMPT is therefore considered to be an attractive target for selective cancer therapy[18-20] and to date, a number of NAMPT inhibitors have been reported. Among these, FK866 (**1**)[21, 22] and CHS828 (**2**)[23, 24] have advanced into phase

II clinical trials (Figure 1A).[25] However, their clinical applications have been restricted due to their dose-limiting thrombocytopenia and gastrointestinal toxicity and other undesirable pharmacokinetic properties.[26, 27] Therefore, there is an urgent need for innovative NAMPT inhibitors with reduced side effects.

EGFR is a member of the ErbB family of receptor tyrosine kinases (RTK) that is a transmembrane protein containing a ligand-binding domain on the external surface of the cytomembrane, a hydrophobic transmembrane region and a tyrosine domain extending into the cytoplasm[28, 29]. Notably, EGFR dysregulation through overexpressions or activating mutations play an important role in tumor development and progression, and has been confirmed to be one of the most valuable targets for the treatment of cancer, especially non-small-cell lung cancer (NSCLC).[30, 31] First-generation inhibitors such as gefitinib (**3**) and erlotinib (**4**) (**Fig. 1**) are currently used as the front-line standard therapy in treating NSCLC patients harboring EGFR activating mutation such as L858R mutation and the exon-19 deletion.[32-35] Despite initial encouraging results, most treated patients eventually relapse and develop secondary or acquired resistance after continuous treatment.[36-38] The most prevalent acquired resistance mechanism is the EGFR mutation T790 M, accounting for 50~60% of the cases[39]. The second-generation irreversible EGFR inhibitors, such as afatinib (**5**)[40-42] and dacomitinib (**6**)[43, 44], and third-generation selective irreversible inhibitors，such as WZ4002 (**7**),[45] osimertinib (**8**)[46, 47] and olmutinib (**9**)[45, 48], have been shown to effectively overcome the resistance induced by a T790M mutation through forming a covalent bond between an inherent electrophilic Michael acceptor

and a conserved Cys797 near the ATP binding domain of EGFR.[49] However, additional resistance rapidly occurs, with one of the potential mechanisms being the appearance of tertiary C797S mutation[50-52]. Therefore, continuous research efforts are urgently needed to discover new drug candidates in order to improve patient outcomes.

We envisioned that the discovery of new chemical entities that are devoid of a Michael acceptor, but active against EGFR T790M mutation should be an effective approach to relieve drug resistance induced by C797S mutation. On the other hand, drug combinations and multitargeted agents have been proposed to combat the acquired resistance and enhance the antitumor efficacy of RTK inhibitors. It has been reported that the growth of EGFR-gene-mutated NSCLC, including activating, T790M and C797S mutations, requires amounts of intracellular ATP to activate EGFR-driven signaling transduction.[53] As described above, NAMPT is fundamentally important in energy generation and maintenance of ATP levels in mammalian cells. Consequently, we postulated that NAMPT inhibitors might be able to synergistically enhance the inhibitory effect of EGFR inhibitors. A single molecule that simultaneously or concurrently can inhibit NAMPT and EGFR enzyme activity would possess a promising anticancer profile. This molecular hybridization strategy that combines two synergistic pharmacophores directly or *via* a linker in order to act on different targets has emerged as a paradigm in drug design. Dual-targeting inhibitors that act by merging the pharmacophore of NAMPT inhibitors into active agents targeting histone deacetylase (HDAC) have been evaluated in cancer treatment.[54, 55]

Herein, we report the first-in-class NAMPT/EGFR bifunctional inhibitors that are structurally lack of a Michael acceptor designed and synthesized on the basis of the aforementioned evidence and multi-targeted drug theory. Particularly, (Z)-2-cyano-1-(6-((4-((3-cyanophenyl)-amino)-7-methoxyquinazolin-6-yl)oxy)pentyl )-3-(pyridin-4-yl)guanidine (**28**) exhibits concurrent inhibition against NAMPT and EGFR with excellent *in vitro* antiproliferative activity and *in vivo* antitumor efficacy.

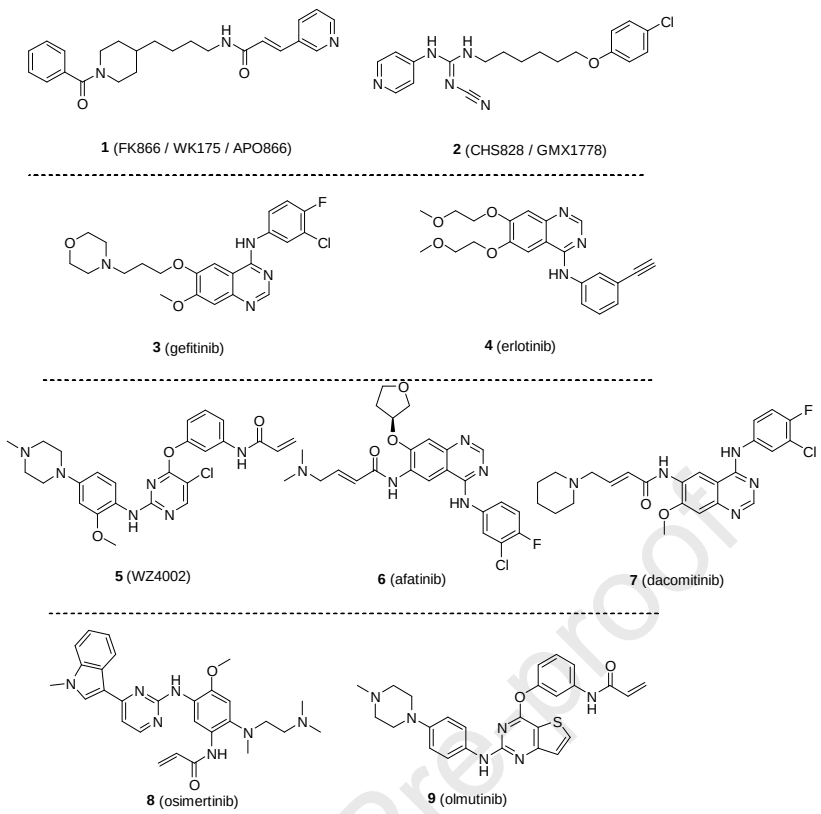


**Fig. 1.** Representative NAMPT and EGFR inhibitors.

## 2. Results and discussion

### *2.1. Rational design of NAMPT/EGFR bifunctional inhibitors*

As shown in **Fig. 2C**, a series of dual NAMPT/EGFR inhibitors were designed utilizing a molecular hybridization strategy. Compared with direct bridging of two inhibitors with a chain linker, a fused pharmacophore is more desirable owing to the likelihood of a lower molecular weight. The NAMPT inhibitor (**2**) and the EGFR inhibitor (**4**) were chosen as the templates for this design. Most NAMPT inhibitors are generally linear and characterized by a widely accepted pharmacophore model containing a cap group mimicking NAM, a connecting unit, a linker and a hydrophobic tail group (**Fig. 2A**) [18, 25]. The cap group combined with the connecting unit constitutes the core, which is important for NAMPT inhibition. The linker should

have an appropriate length and geometry, allowing the tail group to protrude toward the solvent-exposed surface and interact with the hydrophobic amino acids in the rim of the enzyme. However, the tail group can be tolerated since the hydrophobic cleft of the enzyme is large enough to accommodate extraordinarily variable structures.[25, 56] Accordingly, for the NAMPT inhibitor (**2**), the core pyridinylcyanoguanidine motif is indispensable for enzyme inhibitory activity, while the hydrophobic group of **2** can be replaced with a fragment of erlotinib (**4**) to occupy the deep hydrophobic pocket of NAMPT. We explored the erlotinib substructure and found by analysis of the X-ray co-crystal structure of EGFR complexed with erlotinib that it can be modified without sacrificing its EGFR inhibitory activity.

Quinazoline is a privileged skeleton for EGFR inhibitors. From the co-crystal structure of EGFR with erlotinib, we saw that the quinazoline motif occupies the adenine region of the ATP binding pocket and forms two important hydrogen bonds at N1 and N3, and the phenylamino group fits well into the hydrophobic pocket.[57, 58] Therefore, these two moieties cannot be replaced. The ethereal side chains at C-6 and C-7 of the quinazoline ring protrude outward the receptor (**Fig. 2B**).[57, 58] From the perspective of structure-activity relationships (SARs), modification at C-6 and C-7 sites of the quinazoline ring is tolerable and the pharmacophore of **2** introduced to these positions was postulated to retain EGFR/HER2 binding affinity. Meanwhile, the phenylaminoquinazoline backbone of the EGFR inhibitor should fit well into the hydrophobic pocket of the NAMPT enzyme, and the attached side chain with the terminal pyridinylcyanoguanidine was predicted to mimic NAM as required to

suppress the NAMPT activity. Thus, we merged pyridinylcyanoguanidine into the quinazoline pharmacophore of EGFR inhibitor in an attempt to produce, in a single compound, the dual inhibitory activities against NMAPT and EGFR (**Fig. 2C**).

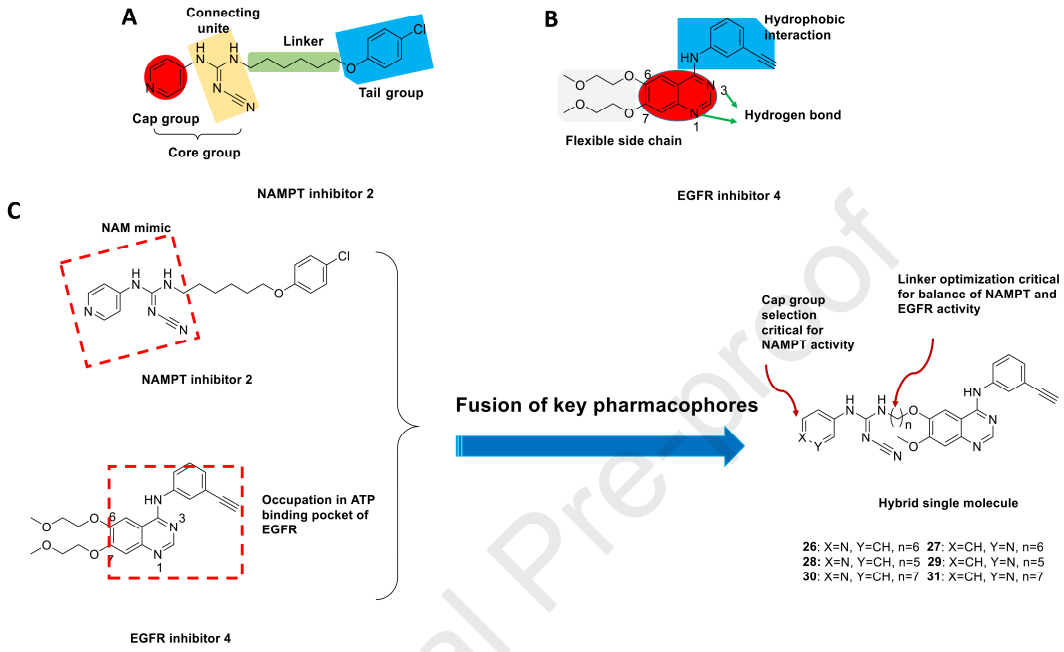


**Fig. 2**. Schematic illustration of the rationale underlying the design of dual NAMPT/EGFR inhibitors. **(A)** Pharmacophore model of NAMPT inhibitor **2**; (B) Pharmacophore model of EGFR inhibitor **4**; (C) The fusion of pharmacophore of NAMPT and EGFR inhibitors.

## *2.2. Chemistry*

The synthetic routes of analogues with various chain lengths and pyridine substitutions are depicted in Schemes 1，2 and 3. The synthesis began with the protection of commercially available starting materials **10**, **11** with a *t*-butyloxycarbonyl (Boc) group. Treatment of **13**-**15** with triphenylphosphine and carbon tetrabromide afforded halohydrocarbons **14** and **15** *via* an Appel reaction. Aminolysis of N-cyanoimido-S,S-dimethyl-dithiocarbonate with primary amines **16**

and **17** in the presence of NaH provided intermediates **18** and **19**, respectively, in good yields.

The quinazoline moiety of erlotinib was prepared from the commercially available compound (**20**), which was first reacted with thionyl chloride using DMF as catalyst to give the 4-chloroquinazoline derivative (**21**). Nucleophilic aromatic substitution of **21** with 3-aminophenylacetylene generated intermediate **22**, which subsequently underwent hydrolysis with ammonium hydroxide to afford an alcohol (**23**).

The target compounds **(26**-**29**) were synthesized as shown in Scheme 2**.** In an alkaline condition, intermediate **23** was installed in the Boc-protected halohydrocarbon amine linkers **14** and **15** to furnish **24** and **25**. Deprotection of compounds **24** and **25** using trifluoroacetic acid, followed by reaction with N'-cyano-N-(pyridine-4-yl)- carbamimidothioate (**18**) or methyl N'-cyano-N-(pyridinyl)-carbamimidothioate (**19**) gave the final products **26**-**29**.

As shown in Scheme 3, compound **23** was coupled with commercially available 7-bromoheptanenitrile to provide an intermediate which has seven methylene spacers, and which was further reacted with $LiAlH_4$ to afford the corresponding amine. Subsequently, treatment of the amine with methyl N'-cyano-N-(pyridine-4-yl)-carbamimidothioate (**18**) or methyl N'-cyano-N-(pyridine-3-yl)carbamimidothioate (**19**) gave the final compounds **30** and **31**, respectively, with good yields.

## Scheme 1. Synthesis of key intermediates 14, 15, 18, 19 and 23[a]

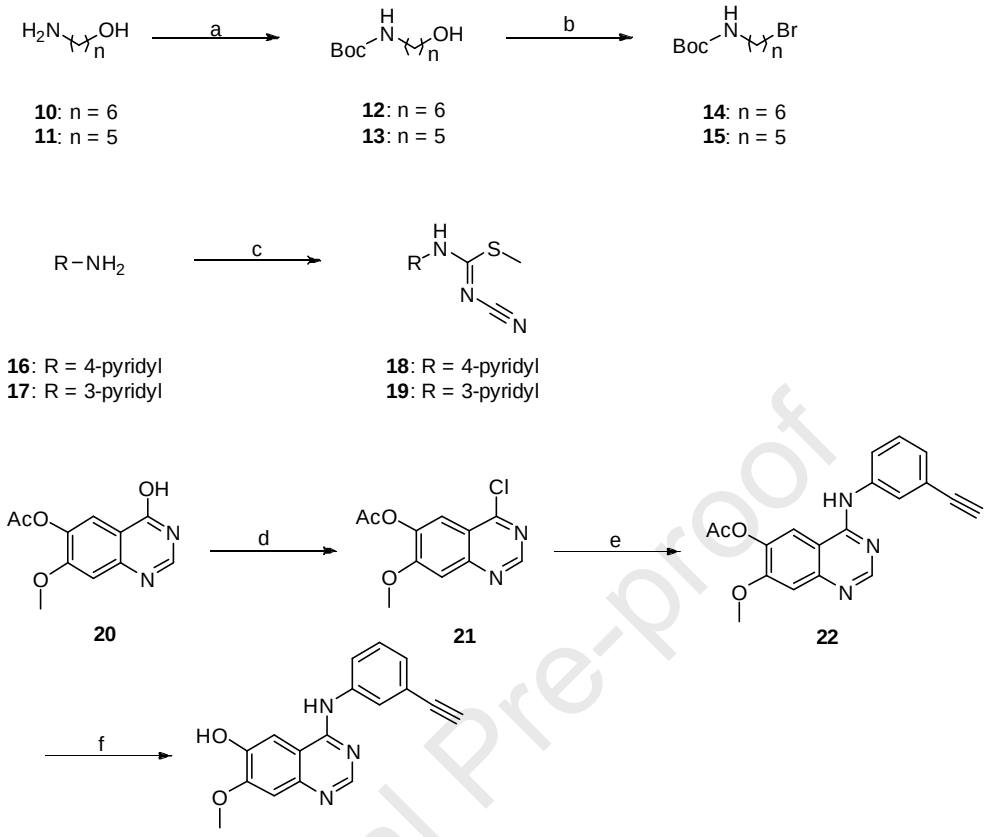


[a] Reagents and conditions: (a) $(Boc)_2O$, DIPEA, DCM, 0 °C - rt, 3 h, 82%; (b) $CBr_4$, $PPh_3$, DCM, 0° C - rt, 16 h, 75% ; (c) NaH, N-cyanoimido-S,S-dimethyl-dithiocarbonate, DMF, 0 °C - rt, 69%; (d) $SOCl_2$, DMF, reflux, overnight, 89%; (e) 3-aminophenylacetylene, isopropanol, reflux, 83%; (f) ammonium hydroxide, MeOH, rt, 90%.

## Scheme 2. Synthesis of target compounds 26-29[a]

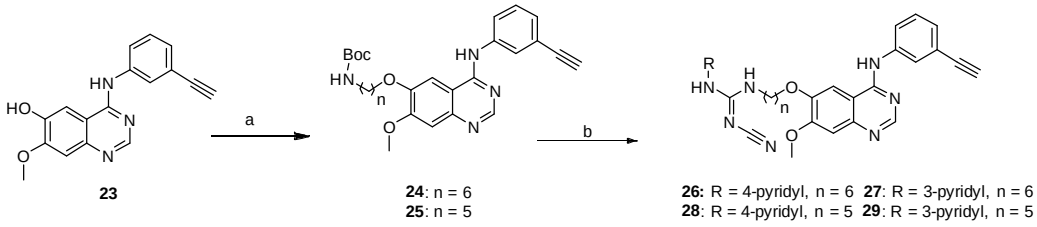


[a] Reagents and conditions: (a) **14-15**, $K_2CO_3$, DMF, 0 °C - rt, 68-85%; (b) (i) TFA, DCM, 0 °C - rt, (ii) **18** or **19**, DMAP, TEA, pyridine, 50 °C, 42-50% in two steps.

**Scheme 3. Synthesis of target compounds 30-31**[a]

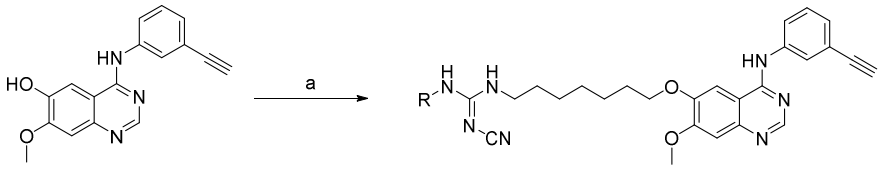


**23** **30**: R = 4-pyridyl, **31**: R = 3-pyridyl

[a] Reagents and conditions: (a) (i) 7-bromoheptanenitrile, $K_2CO_3$, DMF, 0 °C - rt; (ii) $LiAlH_4$, THF, 0 °C - rt; (iii) **18** or **19**, DMAP, TEA, pyridine, 50 °C, 34-41% in three steps.

*2.3. In vitro NAMPT and EGFR inhibition assay*

Initially, we evaluated the inhibitory activities of these compounds against NAMPT, EGFR, $EGFR^{T790M}$, $EGFR^{L861Q}$ and $EGFR^{L858R}$. The results, shown in **Table 1**, showed potency in the nanomolar range against EGFR, $EGFR^{L861Q}$, $EGFR^{L858R}$, $EGFR^{T790M}$ and NAMPT. Retaining the carbon chain length of six methylenes in CHS828 (**2**) in the linking section, compounds **26** and **27** showed excellent inhibitory activity against EGFR, $EGFR^{L861Q}$ and $EGFR^{L858R}$, but somewhat reduced efficacy against NAMPT and $EGFR^{T790M}$. To gain good inhibitory effects against NAMPT and $EGFR^{T790M}$, we attempted to modify the carbon chain linker between the quinazoline C-6 oxygen and the nitrogen atom of pyridinylcyanoguanidine. Lengthening the distance to a seven- methylene spacer led to an NAMPT and $EGFR^{T790M}$ inhibition similar to that of the compound with six methylenes, while shortening the distance to five methylenes yielded a significantly increased NMAPT inhibition (**28**, $IC_{50}$ = 41.2 nM; **29**, $IC_{50}$ = 74 nM), and slightly increased $EGFR^{T790M}$ inhibition (**28**, $IC_{50}$ = 153 nM). In addition, the previous SAR studies of CHS828 (**2**) highlighted the importance of the pyridine ring.[59] Therefore, we further explored the position of the substituent in

**Table 1. *In vitro* NAMPT and EGFR inhibitory activities of the target compounds**

| | NAMPT | | EGFR | | $EGFR^{T790M}$ | $EGFR^{L861Q}$ | $EGFR^{L858R}$ |
|---|---|---|---|---|---|---|---|
| Compounds | $IC_{50}$ (nM) | GlideScore[c] | $IC_{50}$ (nM) | GlideScore | $IC_{50}$ (nM) | $IC_{50}$ (nM) | $IC_{50}$ (nM) |
| **1**(FK866) | 20.7±3.11 | NT | NT[b] | NT | NT | NT | NT |
| **5** (WZ4002) | NT | NT | 4.59±0.46 | NT | 1.98±0.23 | 2.86±0.23 | 4.64±0.33 |
| **26** | 131.0±8.55 | -5.7 | 0.35±0.03 | -10.58 | 323.0±43.5 | 0.36±0.038 | 0.32±0.028 |
| **27** | 133.0±14.3 | -6.47 | 0.32±0.031 | -9.74 | 326.0±39.3 | 0.38±0.029 | 0.38±0.031 |
| **28** | 41.2±3.8 | -8.83 | 0.23±0.014 | -10.42 | 153.0±16.2 | 0.26±0.019 | 0.26±0.015 |
| **29** | 74.0±5.7 | -6.89 | 0.52±0.0 | -9.6 | 228.0±15.8 | 0.46±0.05 | 0.41±0.023 |
| **30** | 154.0±13.8 | -5.98 | 0.473±0.0 | -10.64 | 581.0±34.9 | 0.55±0.049 | 0.46±0.039 |
| **31** | 152.0±15.9 | -4.98 | 0.538±0.0 | -9.14 | 448.0±36.7 | 0.49±0.039 | 0.48±0.061 |

[a] **$IC_{50}$** values represent the mean of at least three independent experiments. [b]NT = not tested. [c]GlideScore was exported from Glide 6.7, lower scores mean higher binding affinity.

pyridyl ring. There was slight difference between 3-pyridyl and 4-pyridyl for both targets with six- or seven- methylene linker (**Table 1**). The 4-pyridyl rather than the 3-pyridyl substitution resulted in potency increase with a spacer of five methylenes. Of all the synthesized compounds, the 4-pyridyl compound (**28**) exhibited the highest potency against EGFR, $EGFR^{L861Q}$, $EGFR^{L858R}$, $EGFR^{T790M}$ and NAMPT.

*2.4. In vitro antiproliferation assay*

Having obtained the potent *in vitro* NAMPT and EGFR inhibitory activities, we further evaluated the antiproliferative activities of these compounds against Huh-7 (human liver cancer), MCF-7 (human breast cancer) and K562 (human myelogenous leukemia) utilizing the CCK8 (Cell Counting Kit-8) assay. As shown in **Table 2**, most of these compounds exhibited excellent inhibitory activity against human cancer cell lines. Among all the tested tumor cell lines, the human breast cancer cell line MCF-7 was the most sensitive to all the compounds, delivering $IC_{50}$ values in the nanomolar range. Despite slight differences in enzyme inhibition between 4-pyridyl and 3-pyridyl analogues, the 4-pyridyl compounds had considerably more antiproliferative activity than the 3-pyridyl compounds in various tumor cell lines. Compound **26** was most active against human myelogenous leukemia k562 cell line with an $IC_{50}$ value of 7.47 nM, and compound **28** was the most potent against the two solid tumor cell lines (Huh-7 and MCF-7).

**Table 2. Antiproliferative activities of compounds 26-31.**

| Compd | $GI_{50}$ (nM)[a] | | |
|---|---|---|---|
| | Huh-7 | K562 | MCF-7 |
| **26** | 1.87±0.17 | 7.47±0.68 | 0.15±0.01 |
| **27** | 8.02±1.10 | 24.6±2.58 | 0.16±0.007 |
| **28** | 1.64±0.13 | 38.0±3.11 | 0.10±0.006 |
| **29** | 62.9±6.92 | 175.0±13.69 | 0.98±0.07 |
| **30** | 1.81±0.15 | 50.9±1.02 | 0.21±0.018 |
| **31** | 9.94±1.21 | 42.1±4.37 | 0.63±0.04 |
| **Taxol** | 7.41±0.96 | 2.76±0.43 | 4.85±0.61 |

[a] **$GI_{50}$** values represent the mean of at least three independent experiments.

*2.5. Molecular Docking*

In an investigation of the binding modes of the target compounds in NAMPT and EGFR, the docking program of Glide 6.7 standard precision model showed that compound **28** could be docked into the active sites of NAMPT and wild-type EGFR. The proposed binding modes of compound **28** in NMAPT and wild-type EGFR are shown in **Fig. 3**. Compound **28** is accommodated very well in the active site of NAMPT. The cap group of **28**, *i.e.*, the (*E*)-2-cyano-1-(pyridin-4-yl)guanidine moiety, has identical interactions with this protein as the corresponding moiety of CHS828 (**2**). The pyridine ring exhibits π-π offset stacking with Phe193, and could also have a hydrogen bond interaction bridged by a water molecule with the protein. The guanidyl group forms double hydrogen bonds with Asp219, while the cyano group forms a

hydrogen bond with Ser275. The tail group of compound **28**, an *N*-(3-ethynylphenyl)quinazolin-4-amine, has hydrophobic interactions with several surrounding residues, including Tyr188, Val 242, Ile309, Ala379 (**Fig. 3**), similar to the interactions between CHS828 and NAMPT.

The docking model demonstrated that the bulky tail group, the erlotinib segment of compound **28** has identical interactions with that of erlotinib in the active site of EGFR as described above (**Fig. 3B**). The head group, the (*E*)-2-cyano-1-(pyridin-4-yl)guanidine moiety, could extend into a hydrophobic subpocket in the cleft of the active site through carbon linkers. In this way, the pyridine moiety may have additional interactions with surrounding residues such as Phe699, Leu834, and Leu838. In addition, the polar 2-cyanoguanidine moiety forms four hydrogen bonds with Lys721, Asp831 and Asn818 (**Fig. 3B**). In general, the docking modes are consistent with the *in vitro* activities.



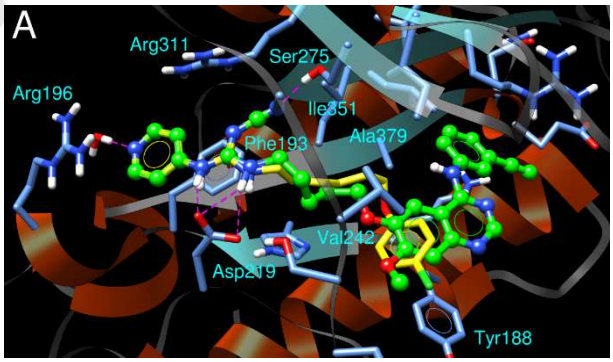

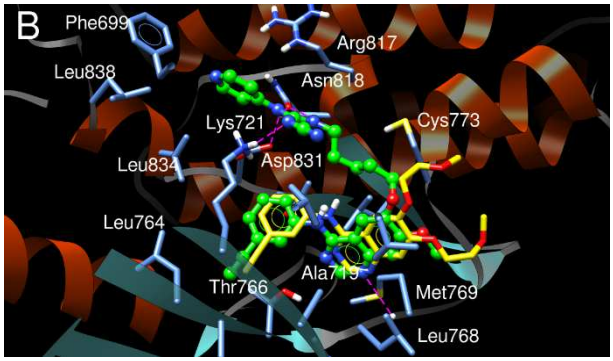


**Fig. 3.** (A) Overlap of the binding modes of CHS828 (green) and compound **28** (yellow) in NAMPT (PDB code 4O12). (B) Overlap of the binding modes of erlotinib (green) and compound **28** (yellow) EGFR (PDB code 4HJO).

*2.6. In vivo antitumor efficacy*

As mentioned above, compound **28** exhibited excellent inhibitory activity toward both NAMPT and EGFR, and more importantly, possessed most potent antiproliferative activity against Huh7 and MCF-7, cell lines which overexpress wild-type EGFR. We further assessed its antiproliferative activity against the H1937 cell line harboring an $EGFR^{L858R/T790M}$ mutation. Compound **28** showed excellent antiproliferative activity against the H1937 cell line with an $IC_{50}$ value of 78.3 nM. The *in vivo* antitumor efficacy of compound **28** in the H1937 xenograft nude mouse model was evaluated. An H1975 lung cancer xenograft nude mouse model was established to evaluate the *in vivo* antitumor potency of compound **28**, and gefitinib, a first-generation EGFR inhibitor was used as a negative control. The BALB/c nude mice were inoculated in the right flank with suspensions of H1975 cells ($3\times10^6$), and when the mean tumor size reached approximately 150 $mm^3$, compound **28** was administered *via i.v.* injection 5 days a week for 3 weeks at a dose of 60 mg/kg. The

results of tumor growth inhibition in different groups at different time points after treatment are shown in **Fig. 4**. Evidently, gefitinib was ineffective against H1937 xenograft (**Fig. 4**) and led to a significant loss of body weight (Fig. S1 in Supporting Information, SI). Compound **28**, however, significantly inhibited the tumor growth at a dose of 60 mg/kg and delivered tumor volume reductions of 75.6%, relative to the control group (**Fig. 4A**). Meanwhile, the tumor weights of mice treated with **28** at 60 mg/kg were reduced by 75% when compared with the control (**Fig. 4B**). In addition, the toxicity of **28** was assessed by monitoring the body weight and survival of the mice. Compound **28** was well tolerated and no significant body weight change was observed in mice treated with **28** during the treatment period (**Fig. S1**).

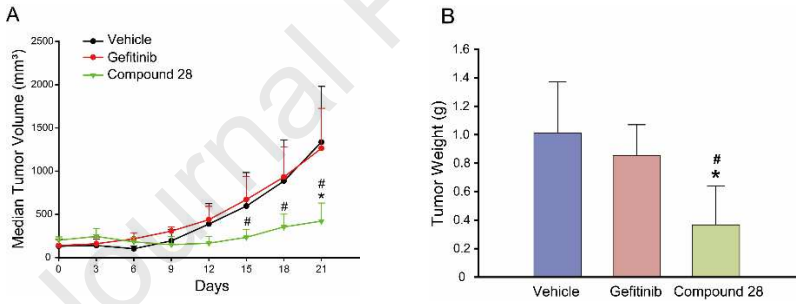


**Fig. 4.** Compound **28** inhibited the growth of implanted H1975 xenograft in nude mice. H1975 tumor-bearing mice were treated with vehicle and **28** (60 mg/kg) with gefitinib (60 mg/kg) as the negative control. (A) Changes in tumor volume of H1975 tumor-bearing mice during 3 weeks treatment. (B) Tumor weight after 3 weeks treatment. Data are expressed as the mean ± standard deviation. Statistical difference was determined by Student's *t*-test. *P<0.05, compared with the vehicle group. #P<0.05, compared with the gefitinib-treated groups.

## 3. Conclusion

Utilizing a pharmacophore merging strategy, we have successfully designed and synthesized a series of first-in-class dual NAMPT/EGFR inhibitors. Optimization of the linker between the quinazoline of erlotinib and the pyridinylcyanoguanidine of

CHS828 led to the identification of compound **28**, a highly effective lead compound with balanced NAMPT and EGFR inhibition. Interestingly, compound **28** exhibited excellent antiproliferative activity in a panel of tumor cell lines, especially breast cancer MCF-7 cell lines at low nanomolar concentrations ($IC_{50}$ = 0.116 nM). Further, it was tested against H1975 xenograft tumors that possess $EGFR^{L858R/T790M}$ mutation in a nude mouse model. The results showed that compound **28** significantly retarded the tumor growth *in vivo*. Third-generation EGFR inhibitors are known to have a Michael receptor warhead component, which can form a covalent bond with the active thiol of Cys797 in the EGFR ATP binding domain.[50] However, mutant EGFR with C797S lacks Cys797 and cannot form a covalent bond with third-generation EGFR inhibitors, which would provide a key mechanism of resistance.[50] Structurally, **28** does not have a Michael receptor but possesses significant efficacy against $EGFR^{L858R/T790M}$ mutation, suggesting its potential to overcome the drug resistance resulting from the T790M mutation.

In conclusion, we have for the first time prepared a dual inhibitor that simultaneously reacts with both NAMPT and EGFR. This is a promising approach to cancer chemotherapy, and further evaluation and optimization of the erlotinib/CHS828 hybrids is now in progress.

## 4. Experimental section

### *4.1. General*

Reagents and solvents from commercial sources were used without further purification. The progress of all reactions was monitored by TLC using

EtOAc/n-hexane as solvent system, and spots were visualized by irradiation with UV light (254 nm) or staining with phosphomolybdic acid. Flash chromatography was performed using silica gel (300−400 mesh). $^{1}$H NMR and $^{13}$C NMR spectra were recorded on a Bruker Avance ARX-400 or a Bruker Avance ARX-500. Chemical shifts δ are reported in ppm, and multiplicity of signals are denoted as: s = singlet, d = doublet, t = triplet and m = multiplet. The low resolution ESIMS was recorded on an Agilent 1200 HPLC-MSD mass spectrometer and the high resolution on an Applied Biosystems Q-STAR Elite ESI-LC-MS/MS mass spectrometer. Anhydrous dichloromethane (DCM) and N,N-dimethylformamide (DMF) were freshly distilled from calcium hydride. All other solvents were reagent grade. All moisture sensitive reactions were carried out in flame dried flask under argon atmosphere. The purity of the final compounds was determined by Agilent 1260 series HPLC system using the following conditions: C-18 column (DicKma, 4.6 mm × 250 mm) with the solvent system (elution conditions: mobile phase A consisting of MeOH; mobile phase B consisting of water containing 0.1% ammonia), with monitoring between 190 and 800 nm. A flow rate of 1.0 mL/min was used. The retention time was reported as $t_R$ (min). The purity of final compounds is > 95%.

*4.2. Experimental procedures*

*4.2.1.*

*2-Cyano-1-(5-((4-((3-ethynylphenyl)amino)-7-methoxyquinazolin-6-yl) oxy)-pentyl)-3-(pyridin-4-yl)guanidine (**28**)*

Trifluoroacetic acid (38 ml) was added dropwise at 0 °C to a solution of **25** (19 g,

38.5 mmol) in anhydrous $CH_2Cl_2$ (150 ml). The reaction mixture was allowed to warm to rt and then stirred until the materials were consumed. The reaction mixture was concentrated *in vacuo* and then saturated $NaHCO_3$ was added. The aqueous layer was extracted twice with $CH_2Cl_2$ (100 ml) and the organic layer washed with brine and dried over anhydrous $Na_2SO_4$. The solvent was removed under vacuum to give the amine as a yellow solid which was used in the next step.

The above intermediate amine was dissolved in pyridine (100 ml), and compound **18** (7.4 g, 38.5 mmol), 4-dimethylaminopyridine (0.46g, 3.8 mmol), triethylamine (10.7 ml, 77.0 mmol) were added. After stirring at 50 °C overnight, the reaction mixture was cooled to rt. The pyridine was evaporated under reduced pressure and then $H_2O$ (100 ml) was added. The aqueous layer was extracted twice with EtOAc (100 ml), and the organic layer washed with brine and dried over anhydrous $Na_2SO_4$, filtered and concentrated under reduced pressure. The resulting mixture was purified by silica column chromatography and eluted with $CH_2Cl_2$/MeOH (40:1) to give **28** (8.4 g, 42% for two steps) as a faint yellow solid. $^1$H NMR (400 MHz, DMSO-$d_6$) $\delta$ 9.47 (s, 1H), 9.38 (s, 1H), 8.49 (s, 1H), 8.37 (s, 2H), 7.98 (s, 1H), 7.89 (d, $J$ = 8.2 Hz, 2H), 7.82 (s, 1H), 7.40 (t, $J$ = 7.9 Hz, 1H), 7.21 (d, $J$ = 9.2 Hz, 4H), 4.18 (s, 1H), 4.15 (d, $J$ = 6.9 Hz, 2H), 3.93 (s, 3H), 3.33 (d, $J$ = 8.2 Hz, 2H), 1.9-1.77 (m, 2H), 1.74-1.58 (m, 2H), 1.53-1.52 (m, 2H). $^{13}$C NMR (125 MHz, DMSO-*d6*) $\delta$ 156.5, 154.9, 153.1, 150.6, 150.0, 148.8, 147.4, 146.2, 140.2, 129.3, 126.8, 125.2, 123.0, 122.1, 116.9, 115.1, 109.3, 107.7, 103.0, 83.9, 80.9, 69.1, 56.3, 42.1, 29.0, 28.7, 23.4. HRMS (ESI) calcd *m/z* for $C_{29}H_{28}N_8O_2$ [$(M + H)^+$] 521.2408, found 521.2405.

*4.2.2.*

*2-Cyano-1-(6-((4-((3-ethynylphenyl)amino)-7-methoxyquinazolin-6-yl)oxy)hexyl)-3-(pyridin-4-yl)guanidine (**26**).*

The procedure used was the same as described above for the synthesis of compound **28**. Compound **26** was obtained as a faint yellow solid (83 mg, 45% for two steps). $^{1}$H NMR (400 MHz, DMSO-$d_6$) $\delta$ 9.56 (s, 1H), 8.50 (s, 1H), 8.38 (d, $J$ = 5.6 Hz, 2H), 7.99 (s, 2H), 7.89 (d, $J$ = 8.3 Hz, 1H), 7.84 (s, 1H), 7.40 (t, $J$ = 7.9 Hz, 1H), 7.31 – 6.99 (m, 4H), 4.19 (s, 1H), 4.15 (t, $J$ = 6.5 Hz, 2H), 3.93 (s, 3H), 3.35-3.30 (m, 2H), 1.91-1.76 (m, 2H), 1.64-1.54 (m, 2H), 1.55-1.33 (m, 4H). $^{13}$C NMR (125 MHz, DMSO-$d_6$) $\delta$ 156.6, 155.0, 152.9, 149.6, 148.8, 146.9, 140.1, 129.3, 126.8, 125.3, 123.1, 122.1, 116.8, 114.9, 109.3, 107.4, 103.0, 83.9, 80.9, 69.2, 56.3, 42.2, 29.0, 29.0, 26.4, 25.7. HRMS (ESI) calcd *m/z* for $C_{30}H_{30}N_8O_2$ [(M + H)$^+$] 535.2565, found 535.2567. HPLC analysis: 99.2% in purity.

*4.2.3.*

*2-Cyano-1-(6-((4-((3-ethynylphenyl)amino)-7-methoxyquinazolin-6-yl)oxy)hexyl)-3-(pyridin-3-yl)guanidine (**27**)*

The procedure was the same as was used for the synthesis of compound **28.** Compound **27** was obtained as a yellow solid (55 mg, 50% for two steps). $^{1}$H NMR (500 MHz, DMSO-$d_6$) $\delta$ 9.50 (s, 1H), 9.20 (s, 1H), 8.49 (s, 1H), 8.46 (d, $J$ = 2.6 Hz, 1H), 8.31 (d, $J$ = 4.7 Hz, 1H), 7.99 (t, $J$ = 1.9 Hz, 1H), 7.89 (dd, $J$ = 8.2, 2.2 Hz, 1H), 7.83 (s, 1H), 7.66 (d, $J$ = 8.2 Hz, 1H), 7.54 (t, $J$ = 5.7 Hz, 1H), 7.39 (t, $J$ = 7.9 Hz, 1H), 7.35 (dd, $J$ = 8.3, 4.7 Hz, 1H), 7.20 (d, $J$ = 11.4 Hz, 2H), 4.18 (s, 1H), 4.14 (t, $J$ = 6.6

Hz, 2H), 3.93 (s, 3H), 3.26 (q, *J* = 6.7 Hz, 2H), 1.84 (d, *J* = 12.1 Hz, 2H), 1.62-1.53 (m, 2H), 1.53-1.45 (m, 2H), 1.41-1.39 (m, 2H). $^{13}$C NMR (125 MHz, DMSO-$d_6$) $\delta$ 158.4, 156.5, 154.9, 153.1, 148.8, 147.3, 145.7, 145.2, 140.2, 135.1, 131.2, 129.3, 126.7, 125.2, 124.0, 123.0, 122.1, 117.4, 109.3, 107.7, 102.9, 83.9, 80.9, 69.2, 56.3, 42.0, 29.2, 29.0, 26.4, 25.7. HRMS (ESI) calcd *m/z* for $C_{30}H_{30}N_8O_2$ [(M + H)$^+$] 535.2565, found 535.2566. HPLC analysis: 95.6% in purity.

*4.2.4.*

*2-Cyano-1-(5-((4-((3-ethynylphenyl)amino)-7-methoxyquinazolin-6-yl)oxy)pentyl)-3-(pyridin-3-yl)guanidine (**29**)*

The procedure was the same as described above for the synthesis of compound **28**. Compound **29** was obtained as a yellow solid (224 mg, 46% for two steps). $^1$H NMR (400 MHz, MeOD) $\delta$ 8.47 (s, 1H), 8.41 (s, 1H), 8.32 (d, *J* = 4.8 Hz, 1H), 7.89 (s, 1H), 7.81-7.70 (m, 2H), 7.66 (s, 1H), 7.39 (dd, *J* = 8.4, 4.9 Hz, 1H), 7.34 (t, *J* = 7.9 Hz, 1H), 7.24 (d, *J* = 7.6 Hz, 1H), 7.08 (s, 1H), 4.16 (t, *J* = 6.2 Hz, 2H), 3.95 (s, 3H), 3.50 (s, 1H), 3.38 (t, *J* = 7.0 Hz, 2H), 1.94-1.91 (m, 2H), 1.74-1.72 (m, 2H), 1.62-1.60 (m, 2H). $^{13}$C NMR (125 MHz, MeOD) $\delta$ 157.0, 155.5, 151.8, 149.3, 145.3, 144.5, 138.9, 134.8, 132.2, 128.4, 127.4, 125.7, 124.0, 123.0, 122.7, 108.9, 105.0, 102.0, 82.8, 77.3, 68.9, 55.2, 41.6, 28.6, 28.3, 23.0. HRMS (ESI) calcd *m/z* for $C_{29}H_{28}N_8O_2$ [(M + H)$^+$] 521.2408, found 521.2411. HPLC analysis: 95.6% in purity.

*4.2.5.*

*2-Cyano-1-(7-((4-((3-ethynylphenyl)amino)-7-methoxyquinazolin-6-yl)oxy)heptyl)-3-(pyridin-4-yl)guanidine (**30**)*

7-bromoheptanenitrile (0.14 ml, 0.95 mmol) and potassium carbonate (218 mg, 1.58 mmol) were added to a stirred solution of compound **23** (230 mg, 0.79 mmol) in DMF (20 ml) and the mixture was stirred for 8 h at rt. DMF was evaporated under reduced pressure and the residue was extracted with EtOAc (30 ml × 3). The combined organic layers were washed with brine, dried over anhydrous $Na_2SO_4$, filtered, and concentrated under reduced pressure. The resulting mixture was purified by silica column chromatograph and eluted with petroleum ether /EtOAc (3 :1) to give the nitrile that was used in the next step.

The above intermediate nitrile was dissolved in anhydrous THF (100 ml) and then $LiAlH_4$ (60 mg, 1.58 mmol) was slowly added at 0 °C under an argon atmosphere. The mixture was stirred for 16 h at rt and then quenched with saturated aqueous $NH_4Cl$ solution and the THF was evaporated under reduced pressure. The residue was extracted with EtOAc (50 ml × 3). The combined organic layers were washed with saturated aqueous $NaHCO_3$ solution and brine, dried over anhydrous $Na_2SO_4$, filtered, and concentrated under reduced pressure. The resulting mixture was purified by silica column chromatography and eluted with petroleum ether/EtOAc (1:1) to give the amine that was used in the next step.

The above intermediate amine was dissolved in pyridine (20 ml), and then compound **18** (151 mg, 0.79 mmol), 4-dimethylaminopyridine (9.6 mg, 0.079 mmol), triethylamine (0.22 ml, 1.58 mmol) were added. After stirring at 50 °C overnight, the reaction mixture was cooled to rt. The pyridine was evaporated under reduced pressure and then $H_2O$ (20 ml) was added. The aqueous layer was extracted twice

with EtOAc (30 ml) and the organic layer washed with brine, dried over anhydrous $Na_2SO_4$, filtered and then concentrated under reduced pressure. The resulting mixture was purified by silica column chromatography and eluted with $CH_2Cl_2$/MeOH (40:1) to give **30** (145 mg, 34% for three steps) as a yellow solid. $^1$H NMR (400 MHz, DMSO-$d_6$) $\delta$ 9.47 (s, 1H), 8.49 (s, 1H), 8.37 (d, $J$ = 5.7 Hz, 2H), 7.99 (s, 2H), 7.89 (d, $J$ = 8.2 Hz, 1H), 7.80 (s, 1H), 7.39 (t, $J$ = 7.9 Hz, 1H), 7.28-7.08 (m, 4H), 4.18 (s, 1H), 4.12 (t, $J$ = 6.5 Hz, 2H), 3.93 (s, 3H), 3.29 (s, 2H), 1.81 (q, $J$ = 7.2, 6.6 Hz, 2H), 1.64-1.29 (m, 8H). $^{13}$C NMR (125 MHz, MeOD) $\delta$ 156.8, 155.3, 152.2, 149.2, 149.0, 147.0, 145.9, 139.2, 128.4, 127.2, 125.5, 122.8, 122.6, 116.5, 114.9, 109.1, 105.6, 101.8, 82.9, 77.3, 68.9, 55.1, 42.0, 28.8, 28.6, 28.5, 26.2, 25.6. HRMS (ESI) calcd *m/z* for $C_{31}H_{32}N_8O_2$ [$(M + H)^+$] 549.2721, found 549.2719. HPLC analysis: 95.9% in purity.

*4.2.6.*

*2-Cyano-1-(7-((4-((3-ethynylphenyl)amino)-7-methoxyquinazolin-6-yl)oxy)heptyl)-3-(pyridin-3-yl)guanidine (**31**)*

The procedure was the same as that described above for the synthesis of compound **30**. Compound **31** was obtained as a yellow solid (90 mg, 41% for two steps). $^1$H NMR (400 MHz, MeOD) $\delta$ 8.50-8.43 (m, 1H), 8.40 (d, $J$ = 1.8 Hz, 1H), 8.33 (d, $J$ = 4.8 Hz, 1H), 7.89 (d, $J$ = 2.3 Hz, 1H), 7.76 (t, $J$ = 8.9 Hz, 2H), 7.67 (d, $J$ = 1.9 Hz, 1H), 7.41 (dd, $J$ = 8.3, 5.0 Hz, 1H), 7.34 (t, $J$ = 7.9 Hz, 1H), 7.24 (d, $J$ = 7.6 Hz, 1H), 7.11 (s, 1H), 4.15 (t, $J$ = 6.0 Hz, 2H), 3.96 (s, 3H), 3.49 (s, 1H), 3.33 (d, $J$ = 7.3 Hz, 2H), 1.91-1.87 (m, 2H), 1.64-1.55 (m, 4H), 1.44-1.41 (m, 4H). $^{13}$C NMR (125 MHz,

MeOD) $\delta$ 158.6, 157.0, 155.4, 152.3, 149.3, 146.1, 145.4, 144.5, 139.2, 134.8, 132.2, 128.4, 127.2, 125.6, 124.0, 122.9, 122.7, 117.2, 109.2, 105.7, 101.9, 82.9, 77.2, 69.0, 55.1, 41.7, 28.8, 28.6, 28.6, 26.2, 25.7. HRMS (ESI) calcd *m/z* for $C_{31}H_{32}N_8O_2$ [(M + H)$^+$] 549.2721, found 549.2725. HPLC analysis: 96.3% in purity.

*4.2.7.*

*tert-Butyl-(5-((4-((3-ethynylphenyl)amino)-7-methoxyquinazolin-6-yl)oxy)pentyl)carbamate (**25**)*

Compound **14** was slowly added at 0 °C to a stirred solution of compound **23** (16.5 g, 56.6 mmol), potassium carbonate (15.6 g, 113.3 mmol) in *N, N*-dimethylformamide (100 ml), then the reaction mixture was allowed to warm to rt. After stirring at rt for 8 h, the solvent was evaporated under reduced pressure. The residue was extracted with EtOAc (80 ml × 3), then the combined organic layers were washed with brine, dried over anhydrous $Na_2SO_4$, filtered and concentrated under reduced pressure. The residue was purified by silica column chromatography and eluted with petroleum ether/EtOAc (1:1) to give **25** (19.0 g, 68%) as a faint yellow solid. $^1$H NMR (400 MHz, $CDCl_3$) $\delta$ 8.66 (d, *J* = 1.8 Hz, 1H), 8.53 (s, 1H), 7.87 (s, 1H), 7.76 (d, *J* = 8.0 Hz, 1H), 7.47 (s, 1H), 7.35-7.19 (m, 3H), 4.77 (s, 1H), 4.00 (t, *J* = 7.0 Hz, 2H), 3.94 (s, 3H), 3.14 (q, *J* = 7.0 Hz, 2H), 3.07 (s, 1H), 1.85-1.81 (m, 2H), 1.53-1.48 (m, 2H), 1.46-1.41 (m, 2H), 1.41 (s, 9H). $^{13}$C NMR (125 MHz, $CDCl_3$) $\delta$ 162.5, 156.5, 155.0, 153.4, 148.7, 147.2, 139.1, 128.8, 127.6, 125.5, 122.7, 122.6, 109.4, 107.5, 101.6, 83.5, 79.5, 77.2, 69.0, 56.1, 39.9, 29.6, 28.4, 27.7, 22.3.

*4.3. Biological assays*

*4.3.1. In vitro NAMPT inhibition assay*

The NAMPT enzyme inhibitory activity was evaluated using a CycLex NAMPT colorimetric assay kit (CycLex NAMPT colorimetric assay kit, MBL International Corp., Woburn, MA) following the instructions of the manufacturer[60]. Assay buffers-1 and -2 were prepared before starting the assay. Assay buffer-1 contains: 10 × NAMPT assay buffer 10 μL, 10 × nicotinamide 10 μL, 10 × PRPP 10 μL, 10 × ATP 10 μL, recombinant NMNAT1 2 μL, $dH_2O$ 48 μL, total volume 90 μL. Assay buffer-2 contains: 50 × WST-1 2 μL, 50 × ADH 2 μL, 50 × diaphorase 2 μL, 10 × EtOH 10 μL, distilled $H_2O$ 4 μL, total volume 20 μL. Recombinant NAMPT (2 μL) and various concentrations of tested compounds or vehicle were added to each well of the microplate, and the reaction was initiated by adding 90 μL of assay buffer-1 to each well and mixing thoroughly followed by incubation at 30 °C for 60 min. Subsequently, assay buffer-2 (20 μL) was added to each well of the microplate and mixed thoroughly. The absorbance at 450 nm was monitored for 30 min at 5 min intervals using a microtiter plate reader.

*4.3.2. In vitro EGFR activity assay*

According to the instructions of manufacturers, wild type and different EGFR mutants (T790M, L858R, L861Q, L858R/T790M) activity were tested using the Z′-Lyte Kinase Assay Kit (Invitrogen).

*4.3.3. Cell culture and cell viability assay*

Cell lines, Huh-7, MCF7and K562 were purchased from Shanghai Cell Bank,

Chinese Academy of Sciences. Cells were routinely grown and maintained in RPMI or DMEM media with 10% FBS and 1% penicillin/streptomycin. All cell lines were incubated in a Thermo/Forma Scientific $CO_2$ water jacketed incubator with 5% $CO_2$ in air at 37 °C. Cell viability assay was determined by the CCK8 (DOjinDo, Japan) assay. Cells were seeded at a density of 400-800 cells/well in 96-well plates and treated with various concentration of tested compounds or vehicle. After 72 h incubation, CCK8 reagent was added and absorbance was measured at 450 nm using Envision 2104 multilabel reader (Perkin Elmer, USA). Dose response curves were plotted to determine the $IC_{50}$ values using Prism 5.0 (GraphPad Software Inc. USA).

*4.3.4. In vivo antitumor efficacy in the H1975 tumor model*

All the procedures for animal handling, care, and the treatment in this study were performed according to the guidelines approved by the Institutional Animal Care and Use Committee (IACUC) of China Pharmaceutical University following the guidelines of the Association for Assessment and Accreditation of Laboratory Animal Care (AAALAC). Female BALB/c nude mice between 4 to 6 weeks of age were housed in individual HEPA-ventilated cages on a 12 hours light–dark cycle at 21-23 °C and 40-60% humidity, and used for tumor xenografts. H1975 lung cancer cells ($3 \times 10^6$) were subcutaneously implanted in the right flanks of nude mice in a volume of 0.1 ml of RPMI-1640 medium, and the mice were observed for 4 weeks. 12 days after the injection of the cells, the xenograft mice were divided into the three group (n= 6 per group) with a similar tumor volume, which reached ~150 $mm^3$. Gefitinib was suspended in 0.9% normal saline and administered once daily (60 mg/kg, i.g.). Compound **28** was suspended in the solution (including 5% ethanol, 5% dimethyl-sulfoxide, 10% Cremophor EL and 80% normal saline) and administered five times every week (60 mg/kg, i.v.). Mice in the vehicle group were given the same solution as that of compound 28 by intravenous injection. Tumor dimensions were measured

daily with calipers, and tumor volumes were calculated by using the formula TV = width$^2$ × length × 0.5. Beginning on Day 0, tumor dimensions and body weight were measured daily during the experiments. Tumor mass weight was measured at the end of the study.

*4.4. Docking Studies*

Compounds were docked into the active sites of NAMPT (PDB code: 4O12[61]) and EGFR (PDB code: 4HJO[58]) employing the program Glide 5.9 of the Schrödinger suite. The structures were downloaded from the Protein Data Bank and prepared using the protein preparation wizard in the Schrödinger suite. The standard precision (SP) mode of Glide was employed. A post docking minimization was carried out for the best 25 poses for each ligand, and the 10 best poses were reported and analyzed.

**Declaration of interest**

The authors declare that they have no conflict of interests.

**Author information**

Corresponding author:

*E-mail:zli@HoustonMethodist.org (Z. Li);

**E-mail: jiangsh9@gmail.com (S. Jiang).

**Author Contributions**

[#]Wanheng Zhang, Kuojun Zhang, Yiwu Yao and Yunyao Liu contributed equally.

**Acknowledgement**

This work was supported by the National Natural Science Foundation (81773559,

21807114), the Double First-Class University Project (CPU2018GY03). This work was also supported by the Houston Methodist Research Institute (HMRI) and foundation (Z. L.). Dr. Dale J. Hamilton is acknowledged for manuscript review.

**Abbreviation used**

DCM, dichloromethane; DIPEA, *N*,*N*´-diisopropylethyl amine; DMAP, 4-dimethylaminopyridine; DMF, *N*,*N*-dimethylformamide; EGF, epidermal growth factor; EGFR, epidermal growth factor receptor; EMT, epithelial-mesenchymal transition; NA, nicotinic acid; NAD, nicotinamide adenine dinucleotide; NAM, nicotinamide; NAMPT, nicotinamide phosphoribosyltransferase; NMN, nicotinamide mononucleotide; NMNAT, nicotinate/nicotinamide mononucleotide adenyltransferase; NR, nicotinamide riboside; NSCLC, non-small cell lung cancer; PARP, poly-ADP-ribose polymerase; PRPP, 5-phosphoribosyl pyrophosphate; RTKs, receptor tyrosine kinases; SAR, structure-activity relationships; SCLC, small cell lung cancer; TEA, triethylamine; TFA, trifluoroacetic acid; THF, tetrahydrofuran; TKIs, tyrosine kinase inhibitors

**References**

1. Anighoro, A.; Bajorath, J.; Rastelli, G. Polypharmacology: challenges and opportunities in drug discovery. *J. Med. Chem.* **2014,** 57, 7874-7887.

2. Peters, J. U. Polypharmacology - foe or friend? *J. Med. Chem.* **2013,** 56, 8955-8971.

3. Boran, A. D.; Iyengar, R. Systems approaches to polypharmacology and drug discovery. *Curr. Opin. Drug Discov. Devel.* **2010,** 13, 297-309.

4. Hopkins, A. L. Network pharmacology: the next paradigm in drug discovery. *Nat. Chem. Biol.* **2008,** 4, 682-690.

5. Vander Heiden, M. G. Targeting cancer metabolism: a therapeutic window opens. *Nat. Rev. Drug Discov.* **2011,** 10, 671-684.

6. Chiarugi, A.; Dolle, C.; Felici, R.; Ziegler, M. The NAD metabolome--a key determinant of cancer cell biology. *Nat. Rev. Cancer* **2012,** 12, 741-752.

7. Magni, G.; Orsomando, G.; Raffelli, N.; Ruggieri, S. Enzymology of mammalian NAD metabolism in health and disease. *Front. Biosci.* **2008,** 13, 6135-6154.

8. Sauve, A. A. NAD+ and vitamin B3: from metabolism to therapies. *J. Pharmacol. Exp. Ther.* **2008,** 324, 883-893.

9. Burgos, E. S. NAMPT in regulated NAD biosynthesis and its pivotal role in human metabolism. *Curr. Med. Chem.* **2011,** 18, 1947-1961.

10. Dahl, T. B.; Holm, S.; Aukrust, P.; Halvorsen, B. Visfatin/NAMPT: a multifaceted molecule with diverse roles in physiology and pathophysiology. *Annu. Rev. Nutr.* **2012,** 32, 229-243.

11. Cerna, D.; Li, H.; Flaherty, S.; Takebe, N.; Coleman, C. N.; Yoo, S. S. Inhibition of nicotinamide phosphoribosyltransferase (NAMPT) activity by small molecule GMX1778 regulates reactive oxygen species (ROS)-mediated cytotoxicity in a p53- and nicotinic acid phosphoribosyltransferase1 (NAPRT1)-dependent manner. *J. Biol. Chem.* **2012,** 287, 22408-22417.

12. Ward, P. S.; Thompson, C. B. Metabolic reprogramming: a cancer hallmark even warburg did not anticipate. *Cancer cell* **2012,** 21, 297-308.

13. Lucas, S.; Soave, C.; Nabil, G.; Ahmed, Z. S. O.; Chen, G.; El-Banna, H. A.; Dou, Q. P.; Wang, J. Pharmacological inhibitors of NAD biosynthesis as potential an-ticancer agents. *Recent Pat. Anticancer Drug Discov.* **2017,** 12, 190-207.

14. Rongvaux, A.; Andris, F.; Van Gool, F.; Leo, O. Reconstructing eukaryotic NAD metabolism. *BioEssays : news and reviews in molecular, cellular and developmental biology* **2003,** 25, 683-690.

15. Gross, J. W.; Rajavel, M.; Grubmeyer, C. Kinetic mechanism of nicotinic acid phosphoribosyltransferase: implications for energy coupling. *Biochemistry* **1998,** 37, 4189-4199.

16. Olesen, U. H.; Hastrup, N.; Sehested, M. Expression patterns of nicotinamide

phosphoribosyltransferase and nicotinic acid phosphoribosyltransferase in human malignant lymphomas. *APMIS : acta pathologica, microbiologica, et immunologica Scandinavica* **2011,** 119, 296-303.

17. Piacente, F.; Caffa, I.; Ravera, S.; Sociali, G.; Passalacqua, M.; Vellone, V. G.; Becherini, P.; Reverberi, D.; Monacelli, F.; Ballestrero, A.; Odetti, P.; Cagnetta, A.; Cea, M.; Nahimana, A.; Duchosal, M.; Bruzzone, S.; Nencioni, A. Nicotinic acid phosphoribosyltransferase regulates cancer cell metabolism, susceptibility to NAMPT inhibitors, and DNA repair. *Cancer Res.* **2017,** 77, 3857-3869.

18. Sampath, D.; Zabka, T. S.; Misner, D. L.; O'Brien, T.; Dragovich, P. S. Inhibition of nicotinamide phosphoribosyltransferase (NAMPT) as a therapeutic strategy in cancer. *Pharmacol. Ther.* **2015,** 151, 16-31.

19. Chen, H.; Wang, S.; Zhang, H.; Nice, E. C.; Huang, C. Nicotinamide phosphoribosyltransferase (Nampt) in carcinogenesis: new clinical opportunities. *Expert Rev. Anticancer Ther.* **2016,** 16, 827-838.

20. Montecucco, F.; Cea, M.; Bauer, I.; Soncini, D.; Caffa, I.; Lasiglie, D.; Nahimana, A.; Uccelli, A.; Bruzzone, S.; Nencioni, A. Nicotinamide phosphoribosyltransferase (NAMPT) inhibitors as therapeutics: rationales, controversies, clinical experience. *Curr. Drug Targets* **2013,** 14, 637-643.

21. Hasmann, M.; Schemainda, I. FK866, a highly specific noncompetitive inhibitor of nicotinamide phosphoribosyltransferase, represents a novel mechanism for induction of tumor cell apoptosis. *Cancer Res.* **2003,** 63, 7436-7442.

22. Nahimana, A.; Attinger, A.; Aubry, D.; Greaney, P.; Ireson, C.; Thougaard, A. V.; Tjornelund, J.; Dawson, K. M.; Dupuis, M.; Duchosal, M. A. The NAD biosynthesis inhibitor APO866 has potent antitumor activity against hematologic malignancies. *Blood* **2009,** 113, 3276-3286.

23. Hovstadius, P.; Larsson, R.; Jonsson, E.; Skov, T.; Kissmeyer, A. M.; Krasilnikoff, K.; Bergh, J.; Karlsson, M. O.; Lonnebo, A.; Ahlgren, J. A Phase I study of CHS 828 in patients with solid tumor malignancy. *Clin. Cancer Res.* **2002,** 8, 2843-2850.

24. Ravaud, A.; Cerny, T.; Terret, C.; Wanders, J.; Bui, B. N.; Hess, D.; Droz, J. P.; Fumoleau, P.; Twelves, C. Phase I study and pharmacokinetic of CHS-828, a

guanidino-containing compound, administered orally as a single dose every 3 weeks in solid tumours: an ECSG/EORTC study. *Eur. J. Cancer* **2005,** 41, 702-707.

25. Galli, U.; Travelli, C.; Massarotti, A.; Fakhfouri, G.; Rahimian, R.; Tron, G. C.; Genazzani, A. A. Medicinal chemistry of nicotinamide phosphoribosyltransferase (NAMPT) inhibitors. *J. Med. Chem.* **2013,** 56, 6279-6296.

26. Holen, K.; Saltz, L. B.; Hollywood, E.; Burk, K.; Hanauske, A. R. The pharmacokinetics, toxicities, and biologic effects of FK866, a nicotinamide adenine dinucleotide biosynthesis inhibitor. *Invest. New Drugs* **2008,** 26, 45-51.

27. von Heideman, A.; Berglund, A.; Larsson, R.; Nygren, P. Safety and efficacy of NAD depleting cancer drugs: results of a phase I clinical trial of CHS 828 and overview of published data. *Cancer Chemother. Pharmacol.* **2010,** 65, 1165-1172.

28. Roskoski, R., Jr. Small molecule inhibitors targeting the EGFR/ErbB family of protein-tyrosine kinases in human cancers. *Pharmacol. Res.* **2018,** 139, 395-411.

29. Roskoski, R., Jr. ErbB/HER protein-tyrosine kinases: structures and small molecule inhibitors. *Pharmacol. Res.* **2014,** 87, 42-59.

30. Sukrithan, V.; Deng, L.; Barbaro, A.; Cheng, H. Emerging drugs for EGFR-mutated non-small cell lung cancer. *Expert Opin. Emerg. Drugs* **2018**, 1-12.

31. Sharma, S. V.; Bell, D. W.; Settleman, J.; Haber, D. A. Epidermal growth factor receptor mutations in lung cancer. *Nat. Rev. Cancer* **2007,** 7, 169-181.

32. Pao, W.; Chmielecki, J. Rational, biologically based treatment of EGFR-mutant non-small-cell lung cancer. *Nat. Rev. Cancer* **2010,** 10, 760-774.

33. Maemondo, M.; Inoue, A.; Kobayashi, K.; Sugawara, S.; Oizumi, S.; Isobe, H.; Gemma, A.; Harada, M.; Yoshizawa, H.; Kinoshita, I.; Fujita, Y.; Okinaga, S.; Hirano, H.; Yoshimori, K.; Harada, T.; Ogura, T.; Ando, M.; Miyazawa, H.; Tanaka, T.; Saijo, Y.; Hagiwara, K.; Morita, S.; Nukiwa, T. Gefitinib or chemotherapy for non-small-cell lung cancer with mutated EGFR. *N. Engl. J. Med.* **2010,** 362, 2380-2388.

34. Brown, T.; Boland, A.; Bagust, A.; Oyee, J.; Hockenhull, J.; Dundar, Y.; Dickson, R.; Ramani, V. S.; Proudlove, C. Gefitinib for the first-line treatment of locally advanced or metastatic non-small cell lung cancer. *Health Technol. Assess.* **2010,** 14, 71-79.

35. McLeod, C.; Bagust, A.; Boland, A.; Hockenhull, J.; Dundar, Y.; Proudlove, C.; Davis, H.; Green, J.; Macbeth, F.; Stevenson, J.; Walley, T.; Dickson, R. Erlotinib for the treatment of relapsed non-small cell lung cancer. *Health Technol. Assess.* **2009,** 13 Suppl 1: 41-47, 41-7.

36. Pao, W.; Miller, V. A.; Politi, K. A.; Riely, G. J.; Somwar, R.; Zakowski, M. F.; Kris, M. G.; Varmus, H. Acquired resistance of lung adenocarcinomas to gefitinib or erlotinib is associated with a second mutation in the EGFR kinase domain. *PLoS Med.* **2005,** 2, e73.

37. Kocher, O. EGFR mutation and resistance of non–small-cell lung cancer to gefitinib. *N. Engl. J. Med.* **1981,** 27, 700-707.

38. Shih, J. Y.; Gow, C. H.; Yang, P. C. EGFR mutation conferring primary resistance to gefitinib in non-small-cell lung cancer. *N. Engl. J. Med.* **2005,** 353, 207-208.

39. Stewart, E. L.; Tan, S. Z.; Liu, G.; Tsao, M. S. Known and putative mechanisms of resistance to EGFR targeted therapies in NSCLC patients with EGFR mutations-a review. *Translational lung cancer research* **2015,** 4, 67-81.

40. Camidge, D. R.; Pao, W.; Sequist, L. V. Acquired resistance to TKIs in solid tumours: learning from lung cancer. *Nat. Rev. Clin. Oncol.* **2014,** 11, 473-481.

41. Ou, S. H. Second-generation irreversible epidermal growth factor receptor (EGFR) tyrosine kinase inhibitors (TKIs): a better mousetrap? A review of the clinical evidence. *Crit. Rev. Oncol. Hematol.* **2012,** 83, 407-421.

42. Li, D.; Ambrogio, L.; Shimamura, T.; Kubo, S.; Takahashi, M.; Chirieac, L. R.; Padera, R. F.; Shapiro, G. I.; Baum, A.; Himmelsbach, F.; Rettig, W. J.; Meyerson, M.; Solca, F.; Greulich, H.; Wong, K. K. BIBW2992, an irreversible EGFR/HER2 inhibitor highly effective in preclinical lung cancer models. *Oncogene* **2008,** 27, 4702-4711.

43. Zugazagoitia, J.; Diaz, A.; Jimenez, E.; Nunez, J. A.; Iglesias, L.; Ponce-Aix, S.; Paz-Ares, L. Second-line treatment of non-small cell lung cancer: focus on the clinical development of dacomitinib. *Front. Med.* **2017,** 4, 36.

44. Gonzales, A. J.; Hook, K. E.; Althaus, I. W.; Ellis, P. A.; Trachet, E.; Delaney, A. M.; Harvey, P. J.; Ellis, T. A.; Amato, D. M.; Nelson, J. M.; Fry, D. W.; Zhu, T.; Loi, C.

M.; Fakhoury, S. A.; Schlosser, K. M.; Sexton, K. E.; Winters, R. T.; Reed, J. E.; Bridges, A. J.; Lettiere, D. J.; Baker, D. A.; Yang, J.; Lee, H. T.; Tecle, H.; Vincent, P. W. Antitumor activity and pharmacokinetic properties of PF-00299804, a second-generation irreversible pan-erbB receptor tyrosine kinase inhibitor. *Mol. Cancer Ther.* **2008,** 7, 1880-1889.

45. Zhou, W.; Ercan, D.; Chen, L.; Yun, C. H.; Li, D.; Capelletti, M.; Cortot, A. B.; Chirieac, L.; Iacob, R. E.; Padera, R.; Engen, J. R.; Wong, K. K.; Eck, M. J.; Gray, N. S.; Janne, P. A. Novel mutant-selective EGFR kinase inhibitors against EGFR T790M. *Nature* **2009,** 462, 1070-1074.

46. Finlay, M. R.; Anderton, M.; Ashton, S.; Ballard, P.; Bethel, P. A.; Box, M. R.; Bradbury, R. H.; Brown, S. J.; Butterworth, S.; Campbell, A.; Chorley, C.; Colclough, N.; Cross, D. A.; Currie, G. S.; Grist, M.; Hassall, L.; Hill, G. B.; James, D.; James, M.; Kemmitt, P.; Klinowska, T.; Lamont, G.; Lamont, S. G.; Martin, N.; McFarland, H. L.; Mellor, M. J.; Orme, J. P.; Perkins, D.; Perkins, P.; Richmond, G.; Smith, P.; Ward, R. A.; Waring, M. J.; Whittaker, D.; Wells, S.; Wrigley, G. L. Discovery of a potent and selective EGFR inhibitor (AZD9291) of both sensitizing and T790M resistance mutations that spares the wild type form of the receptor. *J. Med. Chem.* **2014,** 57, 8249-8267.

47. Cross, D. A.; Ashton, S. E.; Ghiorghiu, S.; Eberlein, C.; Nebhan, C. A.; Spitzler, P. J.; Orme, J. P.; Finlay, M. R.; Ward, R. A.; Mellor, M. J.; Hughes, G.; Rahi, A.; Jacobs, V. N.; Red Brewer, M.; Ichihara, E.; Sun, J.; Jin, H.; Ballard, P.; Al-Kadhimi, K.; Rowlinson, R.; Klinowska, T.; Richmond, G. H.; Cantarini, M.; Kim, D. W.; Ranson, M. R.; Pao, W. AZD9291, an irreversible EGFR TKI, overcomes T790M-mediated resistance to EGFR inhibitors in lung cancer. *Cancer Discov.* **2014,** 4, 1046-1061.

48. Wang, S.; Cang, S.; Liu, D. Third-generation inhibitors targeting EGFR T790M mutation in advanced non-small cell lung cancer. *J. Hematol. Oncol.* **2016,** 9, 34.

49. Solca, F.; Dahl, G.; Zoephel, A.; Bader, G.; Sanderson, M.; Klein, C.; Kraemer, O.; Himmelsbach, F.; Haaksma, E.; Adolf, G. R. Target binding properties and cellular activity of afatinib (BIBW 2992), an irreversible ErbB family blocker. *J. Pharmacol. Exp. Ther.* **2012,** 343, 342-350.

50. Chen, L.; Fu, W.; Zheng, L.; Liu, Z.; Liang, G. Recent progress of small-molecule epidermal growth factor receptor (EGFR) inhibitors against C797S resistance in non-small-cell lung cancer. *J. Med. Chem.* **2018,** 61, 4290-4300.

51. Jia, Y.; Yun, C. H.; Park, E.; Ercan, D.; Manuia, M.; Juarez, J.; Xu, C.; Rhee, K.; Chen, T.; Zhang, H.; Palakurthi, S.; Jang, J.; Lelais, G.; DiDonato, M.; Bursulaya, B.; Michellys, P. Y.; Epple, R.; Marsilje, T. H.; McNeill, M.; Lu, W.; Harris, J.; Bender, S.; Wong, K. K.; Janne, P. A.; Eck, M. J. Overcoming EGFR(T790M) and EGFR(C797S) resistance with mutant-selective allosteric inhibitors. *Nature* **2016,** 534, 129-132.

52. Wang, S.; Tsui, S. T.; Liu, C.; Song, Y.; Liu, D. EGFR C797S mutation mediates resistance to third-generation inhibitors in T790M-positive non-small cell lung cancer. *J. Hematol. Oncol.* **2016,** 9, 59.

53. Okumura, S.; Sasaki, T.; Minami, Y.; Ohsaki, Y. Nicotinamide phosphoribosyltransferase: A potent therapeutic target in non-small cell lung cancer with epidermal growth factor receptor-gene mutation. *J. Thorac. Oncol.* **2012,** 7, 49-56.

54. Dong, G.; Chen, W.; Wang, X.; Yang, X.; Xu, T.; Wang, P.; Zhang, W.; Rao, Y.; Miao, C.; Sheng, C. Small molecule inhibitors simultaneously targeting cancer metabolism and epigenetics: Discovery of novel nicotinamide phosphoribosyltransferase (NAMPT) and histone deacetylase (HDAC) dual inhibitors. *J. Med. Chem.* **2017,** 60, 7965-7983.

55. Chen, W.; Dong, G.; Wu, Y.; Zhang, W.; Miao, C.; Sheng, C. Dual NAMPT/HDAC inhibitors as a new strategy for multitargeting antitumor drug discovery. *ACS Med. Chem. Lett.* **2018,** 9, 34-38.

56. Khan, J. A.; Tao, X.; Tong, L. Molecular basis for the inhibition of human NMPRTase, a novel target for anticancer agents. *Nat. Struct. Mol. Biol.* **2006,** 13, 582-588.

57. Stamos, J.; Sliwkowski, M. X.; Eigenbrot, C. Structure of the epidermal growth factor receptor kinase domain alone and in complex with a 4-anilinoquinazoline inhibitor. *J. Biol. Chem.* **2002,** 277, 46265-46272.

58. Park, J. H.; Liu, Y.; Lemmon, M. A.; Radhakrishnan, R. Erlotinib binds both

inactive and active conformations of the EGFR tyrosine kinase domain. *Biochem. J.* **2012,** 448, 417-423.

59. Schou, C.; Ottosen, E. R.; Petersen, H. J.; Björkling, F.; Latini, S.; Hjarnaa, P. V.; Bramm, E.; Binderup, L. Novel cyanoguanidines with potent oral antitumour activity. *Bioorg. Med. Chem. Lett.* **1997,** 7, 3095-3100.

60. Bai, J.; Liao, C.; Liu, Y.; Qin, X.; Chen, J.; Qiu, Y.; Qin, D.; Li, Z.; Tu, Z. C.; Jiang, S. Structure-based design of potent nicotinamide phosphoribosyltransferase inhibitors with promising in vitro and in vivo antitumor activities. *J. Med. Chem.* **2016,** 59, 5766-5779.

61. Oh, A.; Ho, Y. C.; Zak, M.; Liu, Y.; Chen, X.; Yuen, P. W.; Zheng, X.; Liu, Y.; Dragovich, P. S.; Wang, W. Structural and biochemical analyses of the catalysis and potency impact of inhibitor phosphoribosylation by human nicotinamide phosphoribosyltransferase. *Chembiochem : a European journal of chemical biology* **2014,** 15, 1121-1130.



**Graphical abstract**

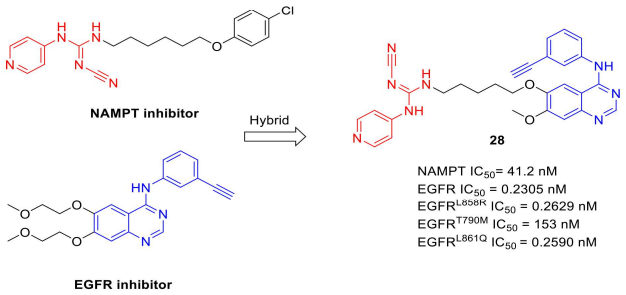


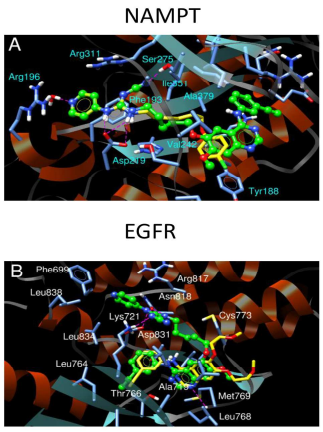

**Dual Nicotinamide Phosphoribosyltransferase and Epidermal Growth Factor Receptor Inhibitors for the Treatment of Cancer**

**Highlight**

- The discovery of multitarget drugs has emerged as a research hotspot in modern anticancer therapy.
- A series of first-in-class dual inhibitors simultaneously targeting EGFR and NAMPT have been identified.
- The most active compound **28** showed dual balanced inhibitory activity towards EGFR and NAMPT *in vitro*.
- The most active compound **28** imparted excellent antiproliferative activity against several cancer cell lines.
- The most active compound **28** exhibited good *in vivo* antitumor efficacy in a human NSCLC (H1975) xenograft nude mouse model.

The authors declared that the work described has not been published previously (except in the form of an abstract, a published lecture or academic thesis), that it is not under consideration for publication elsewhere, that its publication is approved by all authors and tacitly or explicitly by the responsible authorities where the work was carried out, and that, if accepted, it will not be published elsewhere in the same form, in English or in any other language, including electronically without the written consent of the copyright-holder.